Integration concept of an Electron Cyclotron System in DEMO

Integration concept of an Electron Cyclotron System in DEMO

T. Franke[1,2], G. Aiello[3], K. Avramidis[4], C. Bachmann[1], B. Baiocchi[5], C. Baylard[1], A. Bruschi[5], D. Chauvin[1], A. Cufar[6], R. Chavan[7], C. Gliss[1], F. Fanale[5], L. Figini[5], G. Gantenbein[4], S. Garavaglia[5], G. Granucci[5], J. Jelonnek[4], G. Suárez López[2], A. Moro[5], M. Moscheni[8], N. Rispoli[5], M. Siccinio[1,2], P. Spaeh[3], D. Strauss[3], F. Subba[8], I. Tigelis[9], M. Q. Tran[7], C. Tsironis[10], C. Wu[4], H. Zohm[2]

[1]EUROfusion Consortium, Boltzmannstr. 2, D-85748 Garching, Germany,
[2]Max-Planck-Institut für Plasmaphysik, Boltzmannstr. 2, D-85748 Garching, Germany,
[3]IAM-AWP, Karlsruhe Institute of Technology (KIT), Kaiserstr. 12, 76131 Karlsruhe, Germany,
[4]IHM, Karlsruhe Institute of Technology (KIT), Kaiserstr. 12, 76131 Karlsruhe, Germany,
[5]Institute for Plasma Science and Technology, National Research Council (ISTP-CNR), via Cozzi 53, 20125 Milan, Italy,
[6]Reactor Physics Department, Jožef Stefan Institute, Jamova cesta 39, SI-1000, Ljubljana, Slovenia,
[7]SPC Swiss Plasma Center (SPC), EPFL, CH-1015 Lausanne, Switzerland,
[8]NEMO Group, Dipartimento Energia, Politecnico di Torino, Corso Duca degli Abruzzi 24, 10129, Turin, Italy,
[9]National and Kapodistrian University of Athens, Department of Physics, Zografou, GR-157 84, Athens, Greece,
[10]School of Electrical and Computer Engineering, National Technical University of Athens, 157 73 Athens, Greece.

The pre-conceptual layout for an electron cyclotron system (ECS) in DEMO is described. The present DEMO ECS considers only equatorial ports for both plasma heating and neoclassical tearing mode (NTM) control. This differs from ITER, where four launchers in upper oblique ports are dedicated to NTM control and one equatorial EC port for heating and current drive (H&CD) purposes as basic configuration. Rather than upper oblique ports, DEMO has upper vertical ports to allow the vertical removal of the large breeding blanket segments. While ITER is using front steering antennas for NTM control, in DEMO the antennas are recessed behind the breeding blanket and called mid-steering antennas, referred to the radially recessed position to the breeding blanket.

In the DEMO pre-conceptual design phase two variants are studied to integrate the ECS in equatorial ports. The first option integrates waveguide bundles at four vertical levels inside EC port plugs with antennas with fixed and movable mid-steering mirrors that are powered by gyrotrons, operating at minimum two different multiples of the fundamental resonance frequency of the microwave output window. Alternatively, the second option integrates fixed antenna launchers connected to frequency step-tunable gyrotrons. The first variant is described in this paper, introducing the design and functional requirements, presenting the equatorial port allocation, the port plug design including its maintenance concept, the basic port cell layout, the transmission line system with diamond windows from the tokamak up to the RF building and the gyrotron sources.

The ECS design studies are supported by neutronic and tokamak integration studies, quasi-optical and plasma physics studies, which will be summarized. Physics and technological gaps will be discussed and an outlook to future work will be given.

Keywords: Electron Cyclotron, Heating & Current Drive, Port Integration, DEMO

1. Introduction

The pre-conceptual layout for an electron cyclotron system (ECS) in DEMO is described, which shows the integration of the EC (electron cyclotron) EPP (equatorial port plug) in the tokamak. The work was carried out by DEMO PMI (central team) and the work package heating & current drive (WPHCD) in collaboration. The present DEMO ECS considers only equatorial ports for plasma heating, neoclassical tearing mode (NTM) control and radiative instability control. This differs from ITER, where four launchers in upper oblique ports are dedicated to NTM control and one equatorial EC port for heating and current drive (H&CD) purposes as basic configuration. Rather than upper oblique ports, DEMO has upper vertical ports to allow the vertical removal of the large breeding blanket (BB) segments. While ITER is using front steering antennas (FSAs) for NTM control, in DEMO the antennas are recessed behind the BB and called mid-steering antennas (MSAs), referred to the radially recessed position to the BB. Remote steering antennas (RSAs) were abandoned from review panel of the work package HCD for DEMO, because they are space-consuming, expensive in development, and have beam size requirement issues.

The paper describes the design of the EC port and port plug (launcher), which was presented in preparation for the DEMO Gate 1 Review [1], as part of the justification dossiers.

The first EC EPP design based on the MSA concept was proposed in 2019. In 2020 the design was upgraded and further refined based on first verification results of the 2019 design. The new model is similar in the general layout and the main strategy is to split the port plug into two halves, one containing only the fixed mirrors (FMs) and the other one with movable or steering mirrors (SMs) and also with actuators to steer them. The assumption was made, that the FM port plug module will be a lifetime component, being more shielded and also having no active movable components, whereas the SM

author's email: thomas.franke@euro-fusion.org

port plug module would need exchanges for regular maintenance during lifetime once the neutron damage limits of the materials (displacement per atom (dpa) in structural components) or operational lifetime limits of actuators would be reached.

The 2020 design of the DEMO EC EPP integrated in the tokamak can be seen in Fig. 1. This ECS variant is called ECS.FF, were FF stands for fixed frequencies (for this version it is planned to use 2 frequency gyrotrons) is not tunable and instead the plasma facing mirrors are steered. An alternative option of the ECS launchers for a system without movable mirrors but solely based on the tuning of the gyrotrons frequency is the ECS.TF (tunable frequencies) system, described in [2][3].

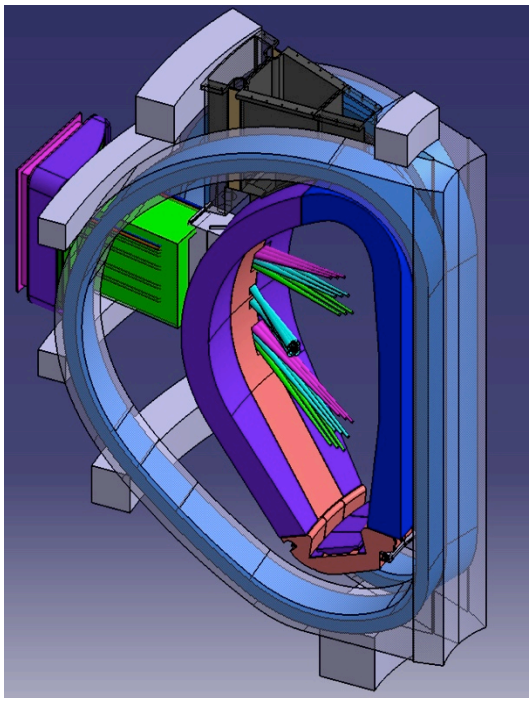

Fig. 1. 2020 design of the DEMO EC MSA launcher with mm wave beam trajectories.

2. Requirements

A mature design has to start from the requirements. Several types of requirements have to be considered, namely for the ECS design they are:

i. The stakeholder and overarching requirements, namely the EUROfusion roadmap of 2013 [4] and its update in 2018 [5], the DEMO stakeholder requirements are given in [6], and the plant requirement document which gives the general DEMO plant requirements, see [7].

ii. The physics requirements which are the 2018 DEMO physics baseline [8][9] and the top level HCD system requirement document (SRD) from 2020 [10].

iii. The engineering baseline and its requirements as described in [11][12].

iv. Further requirements are of more technical nature, as they are layout and actuator requirements, efficiency, tritium breeding ratio (TBR) and reliability, availability, maintainability and inspectability (RAMI) requirements, structural and geometrical and mass requirements, as well as vacuum and neutron shielding requirements. For more details on the requirements mentioned under (iii) please refer to [13]. Also there are the main interfaces listed.

The EC system is in charge of key functions as initiating, sustaining and assisting the tokamak plasma discharge. The main tasks can be performed launching the required power, concentrated in narrow converging or diverging beams, from the EC launcher to specific deposition regions in the plasma, with a prescribed power, width and with a certain frequency. Main EC functions are:

- assisted plasma break-down (5 – 8 MW)
- start-up, ramp-up to burn (min. ~70 MW [14])
- MHD (NTM) control (~30 MW)
- Bulk heating (BH) of core plasma (~30 MW)
- radiative instability (RI) control (~70 MW)
- ramp-down (power similar to ramp-up power)

These are provisional assumptions from DEMO physics, for ramp-up and ramp-down trajectories and perturbations cf. [15]. They are under further elaboration together with the plasma scenario for DEMO.

In Fig. 2 the trajectories of the EC beams are shown for the different functions. The poloidal cross-sections of the DEMO plasma flux surfaces (in grey) are shown together with the beam trajectories (in blue) and the resonance locations (in solid orange the "cold plasma" resonance and in dashed orange the "hot plasma" resonance), determining different power deposition localization by the different resonance position of the beam with the plasma. The launch parameters (steering angles) and frequencies are reported on top of each figure: in the left and the middle figures the positions of the two main NTM instabilities (on the flux surfaces characterized by q = 1.5 and q = 2) are shown in green. The figure at left is an example of power deposition on an NTM instability (on the green line), while the central and right ones are examples respectively of BH (at plasma center) and heating at plasma edge for RI control. This last is addressed in [16][17].

In Fig. 2 specific positions have been used for launch of the beams from mirrors located in the EC equatorial port plug. For NTM stabilization the launch has been placed in the top part of the EC port plug, which is closer to the upper crossing of the resonance with the NTM (a launch at the bottom toward the lower crossing would be convenient as well and was therefore integrated in the port plug design, not shown in Fig. 2). Two main gyrotrons frequencies are to be selected among the triplet of 136 GHz, 170 GHz and 204 GHz for an optimized 2-frequency gyrotrons [18][19][20]. The EC power shall be provided from 2-frequency coaxial multi-purpose 2 MW gyrotrons, which are also under development for

DEMO. Once the frequency of the wave is fixed for a given plasma condition, the electron cyclotron resonance position or deposition localization can be chosen by changing the beam launch angle by tilting the last mirror. The deposition location occurs at the crossing of beams with the EC resonance.

Recently a new function had been added, which is the radiative instability control (RI) event handling. This event can be caused by small particles eroded from the first wall (FW) or other plasma facing components like limiters causing a thermal instability event by large power radiation.

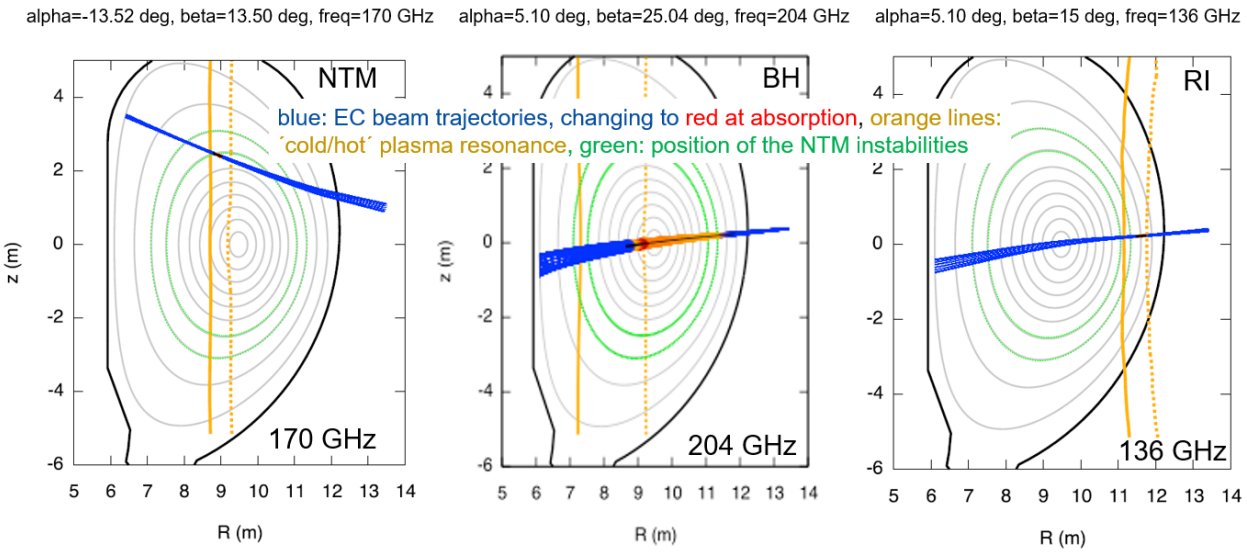

Fig. 2. Poloidal cross-sections of the DEMO plasma shown together with the beam trajectories. On top of each figure, the ´alpha´ stands for the poloidal and ´beta´ for the toroidal steering angles.

3. Optical layout

The optical layout is the basis for the structure of the EC EPP. The optical layout is based on the definition of the DEMO directions of the toroidal magnetic field B_t and plasma current I_P [21], both being clockwise when viewed from the top of the machine. The optical layout is driven by physics requirements, beam focalization, NTM islands positions and steering ranges. A toroidal inclination for sufficient local ECCD efficiency is important. The effects of EC beam broadening by plasma density fluctuations are still under study for NTM control and could change the strategy of island control [22][23].

The ideal position for the NTM launch would be still at a higher vertical (z-axis) position, from an upper oblique port as in ITER [24][25], but this type of port is not foreseen in DEMO due to the vertical port architecture for the BB removal. Another advantage of such an upper launching position is that it could minimize the possible effects of beam broadening due to turbulence as mentioned before.

The central part of the equatorial port plug is reserved for launch at the plasma center and at the edge (this requires using another frequency, with resonance located at plasma edge, see [16]).

Also a specific degree of convergence has been used for the beams: For NTMs the deposition region is very small (full width at 1/e in power of 6 cm at the corresponding surfaces in green, [26]), requiring a converging beam, which (for the laws of beam-optics) requires a large focusing mirror to be realized. For BH and RI control, the requirement of convergence is much less strict, so smaller mirrors can be used.

As a last characteristic, since the position of the NTM instability may change over time, the mirrors should be steered to track it, while the BH and RI do not require mirror steering. The optical design of the launcher is made based on the above detailed principles. Two movable large mirrors at the top and bottom of the equatorial port plug, carrying three beams each, aim at the upper and lower NTM positions (in Fig. 1 the central and extreme positions for the waves steered by the mirrors are shown in light blue, green and magenta). Two smaller mirrors, carrying 8 beams each, are located closer to the equatorial plane and aim at the plasma center, to be used for BH and RI control (this last at a different source frequency) (in Fig. 1 shown as blue waves coming out at the mid-plane from the central BB openings).

In all cases the quasi-optical beams are originating from the opening of a waveguide (a metallic cylinder with a small corrugation inside), which is located in the port interior, in specific positions. The beams then reflect on two metallic mirrors M1 and M2 (see Fig. 3), one of which (M2) acts like a lens for converging the beams going into the plasma. In Fig. 3a,b the beams for NTM control, and in Fig. 3c for BH and RI control expands out of the waveguides and are re-directed to the plasma with a proper direction and shape.

The dogleg formed by the mirrors protects from direct neutron streaming into the waveguides, and the layout

has been conceived as made by two different launcher sections, (one for M1 and the second for M2 mirrors) in order to be as compatible as possible with the extraction of one section leaving the other one in place. The waveguide routing was in fact realized on one side of the port, to leave space for remote maintenance extraction of the port plug segment with the launching or steerable mirrors (M2) and thus without removing the waveguides and port plug segment with the fixed mirrors (M1). The reason behind is that the mirrors M2 are subject to more neutron damage as they are facing the plasma directly.

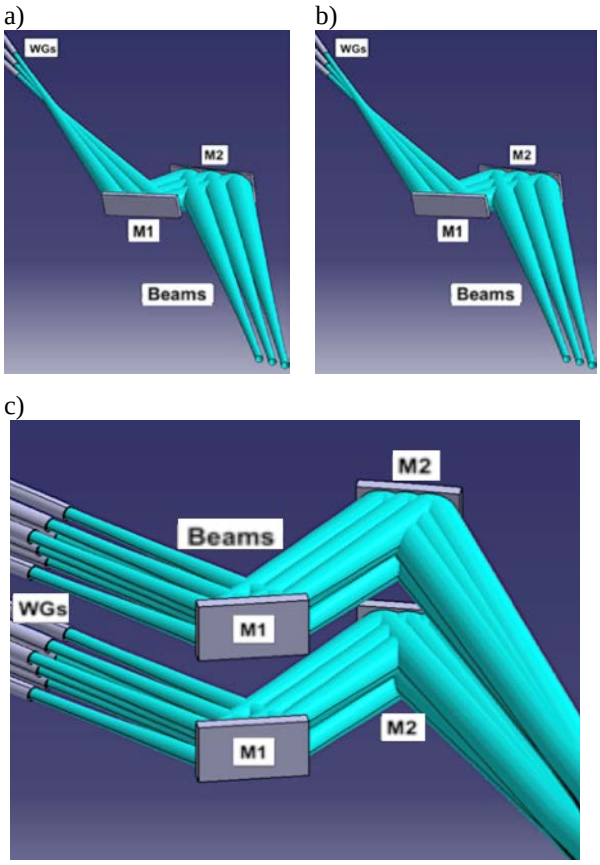

Fig. 3. Optical layout of the EC EPP mirror system, with beam trajectories represented by stigmatic Gaussian beam profiles (conical envelopes). The EC EPP has 4 rows. Fig. 3 a,b. mirror system (M1, M2 fixed) for heating 2 rows x 8 beams x ~2 MW per beam, Fig. 3 c. mirror system (M1 fixed, M2 steerable) and beam paths for NTM control, used as upper and lower rows in the EC EPP, 2 rows x 3 beams x ~2 MW per beam.

4. EC Equatorial Port Plug (EC EPP) design

The mirrors of the in-vessel millimetre wave system require precise alignment and safe installation into the DEMO equatorial port. Thus, they are mounted into dedicated port plugs, which are basically massive structural components with customized shapes and cut-outs which do guarantee undisturbed beam propagation into the plasma, maximum neutron shielding capability and straightforward maintenance processes. Due to their position close to the plasma as well as for bake out active cooling of the plugs will be required.

One single port plug, having installed all eight in-vessel mirrors and filling up the entire front section of the port would be the optimum design with respect to shielding capability and mirror alignment, but has some disadvantages regarding various remote handling classifications expected for the SMs and the FMs, respectively. In addition, the mass of such a full-size port plug would be more than 70 tons, which makes any manipulation by maintenance robots more challenging.

Thus a concept with two separated port plugs has been established (see Fig. 4). One port plug on the left hand side (looking towards the plasma) carries the (M2) mirrors which reflect the beams finally into the plasma. The port plug on the right hand side features the plane (M1) mirrors, which provide the dog-leg configuration of the beam layout. The gap between the two port plugs is also shaped with a small dogleg of 20 mm overlap in order to mitigate neutron streaming between the port plugs (cf. Fig. 5). The consequences of this multi-staged port plug layout for the mirror alignment (and thus the need for additional adjustment mechanisms) will require future analysis, however. As mentioned before, the FM module is a semi-permanent part with waveguides further shielded behind it. Behind the SM module there is empty space in the port cell for easier access by RM tools.

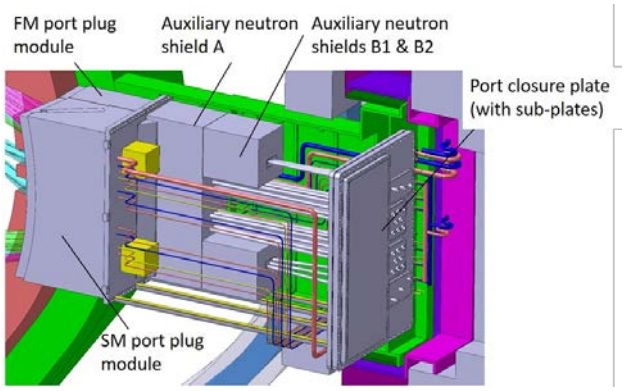

Fig. 4. Isometric view from bioshield side on the EC EPP with FM, SM port plug modules, auxiliary neutron shields and vacuum port closure plate and sub-plates marked, pipes are permanent running along the port side walls.

In 2019 a first design was made for the EC EPP and in 2020 an upgraded design was presented. The improvements of the 2020 design compared to the 2019 design are:

i. better neutronics shielding by e.g. adding of doglegs and extended neutron shields,

ii. improved physics performance achieved by e.g. adapting steering ranges and launching angles and

iii. maintenance recommendations included by e.g. routing of cooling pipes from one only side of the port and the inclusion of actuator space reservations for studies on their positions.

5. EC port design

One of the most important design considerations for the DEMO ports comes from the requirements on the BB

cut-outs. In contrast to ITER or other tokamaks, the equatorial ports are not located in the centre of each tokamak sector, i.e. in the exact middle between two toroidal field coils (TFCs), but they are toroidally shifted, so that the opening of the BB is in the middle of two adjacent blankets. Therefore the port is narrower to one TFC but on the contrary has more space for installations on the other side and other neighbouring TFC, see Fig. 5.

The second consequence from the BB opening restrictions is that the opening for the launching waves has to be designed rectangular and vertically slim but not square shaped.

Behind the BB is the vacuum vessel with the equatorial port extensions attached, sharing the same cooling water. Ribs, as can be seen in Fig. 6 allow for sufficient mechanical stiffness of the port structure.

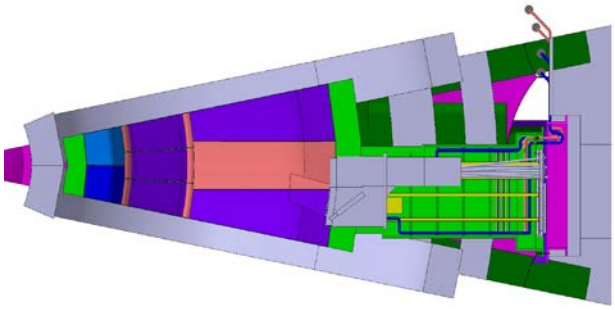

Fig. 5. Toroidal view of EC EPP, port shifted off toroidally from sector centre line.

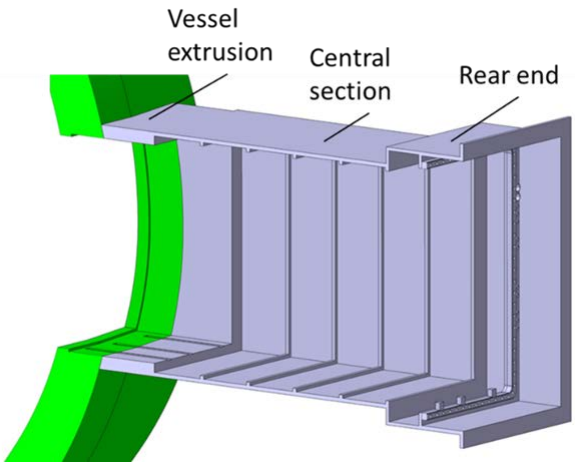

Fig. 6. EC Launcher equatorial port with port extension and ribs.

6. Building integration and port cell layout

For the 2019 design task the building configuration was not taken into account for the structural system of the EC port due to the dominant geometrical constraints of the clearance between the TFCs and poloidal field coils (PFCs). In the 2020 design task the interfaces between the integrated port and the building were analysed on a preliminary basis. The EC port is located at the equatorial port level (or level L1) of the tokamak building.

The building integration is of major importance and going hand in hand with the remote maintenance to make sure, that all the components can be assembled and disassembled for repair or replacement with space sufficient for the main components and the remote maintenance tools.

7. Waveguides

The connection of the in-vessel waveguides with the waveguides out of the port, aligned on the right wall of the port cell, is made through a dogleg path that includes the gate valves and the windows, for each line, see Fig. 7. The path close to the right wall leaves the space for the extraction of the M2 mirrors section, i.e. the steering mirror port plug at the left of each of the EC port plug, see Fig. 8. More details can be found in [16].

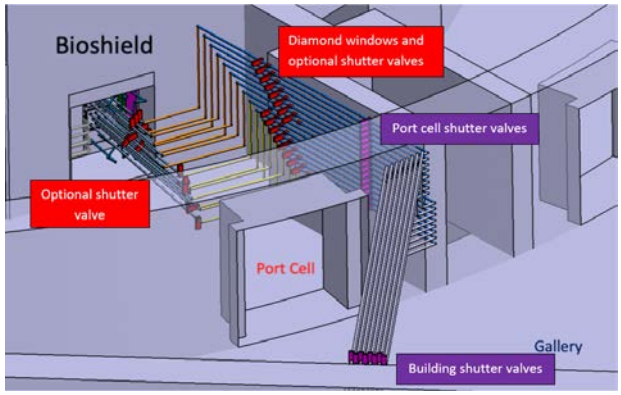

Fig. 7. Waveguide layout in the EP launcher outside region, in the port cell and gallery. Waveguide trajectories are studied for the minimum impact on the space in the port cell and gallery, and on remote maintenance of the steerable (M2) mirror port plug section. Please note that the bioshield plug and the port cell door are not shown.

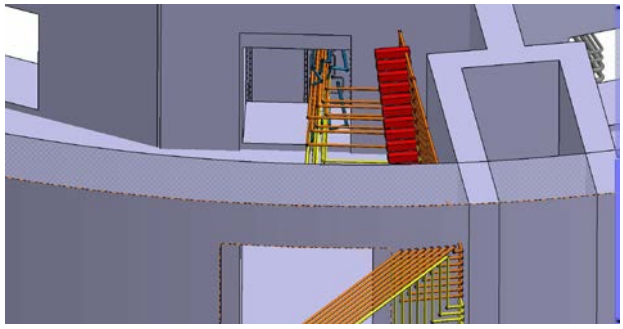

Fig. 8. Port plug removal space of the steerable mirror port plug on the left side of the waveguide bundles. Please note that the bioshield plug and the port cell door are not shown.

8. Windows

The chemical vapour deposition (CVD) diamond windows of the transmission lines are not part of the port integrated design described here, since they are to be placed outside of the port in the EC port cell. They will be installed behind dog-legs of the EC beam transmission system and behind mitre-bends of the transmission line so that neutron streaming to the windows is reduced as much as possible. Since they are a kind of ´far´ interfaces they are just mentioned here for

completeness but any direct neutron-streaming path to the windows is to be avoided and also it should be considered to achieve the easiest access to them for remote maintenance. There are two types of CVD diamond windows considered:

i. for the ECS-FF launcher variant, the fixed frequencies ITER-like disk window [27] perpendicular to the beam transmission, but adapted to the 63.5 mm waveguide inner diameter (50 mm in ITER) and also to the disk resonant thickness for the main frequencies of interest (e.g., 1.85 mm for 170/204 GHz);

ii. for the launcher variant ECS-TF with tunable frequencies, instead the so-called Brewster-angle broadband window which is required for the step-frequency tunable gyrotron operation with a very large disk diameter (minimum 180 mm) being 67.2° the Brewster-angle for diamond [28].

9. Analyses results

9.1 Neutron loads

The material used for the neutronics assessment was defined for each component, in some cases options were given, in order to allow scoping studies [29]. The DEMO PDD [30] suggests dpa´s or the fluencies to be used for main materials for the design of EC port plug as e.g. EUROFER, stainless steel and CuCrZr, knowing that some of the data are to be validated further by e.g. the DEMO oriented neutron source (DONES) [31]. EUROFER is used whenever the activation would be so high, that stainless steel would make an issue for the radiation waste of the DEMO tokamak or where its dpa would be excessive.

Neutronics studies were performed with the 2019 EC port design to assess the suitability of the design in terms of the shielding performance and in terms of the expected nuclear loads in port components. The results include nuclear heating of the TFCs, neutron flux in various parts of the geometry, neutron-induced damage (dpa) in exposed components, nuclear heating maps, and shutdown dose rates. These results are described in more detail in reports [32][33][34]. These results were recently updated for the 2020 EC EPP design and the new results, are better and show reduced heating and dpa values, as expected, by further adding of neutron shielding [35].

An important aspect of the launcher is the design of the neutron-exposed mirrors located in the SM module. Nuclear loads in these mirrors were assessed and are presented in Fig. 9 below. As can be seen, more exposed parts of the mirrors to the plasma receive significantly higher loads than parts located further inside the opening. The mirrors in the model consist of two parts – coating and the body. The body of the steering mirrors is modelled as 19 mm of (40%) water and (60%) steel mixture and the body of the heating mirrors is modelled as 55 mm of (40%) water and (60%) steel mixture. The coating for both types of mirrors is modelled as 5 mm of tungsten. Also for the mirrors the assumption of the design was to use a full CuCrZr mirror instead or a CuCrZr coating to have a better electrical conductivity for the EC waves, but for the latter, the dpa values would be around 3 times as high as for the tungsten coating. This option needs to be further studied. Also the use of tungsten wire re-enforced CuCrZr was discussed but so far it is too early for including such novel materials in the design.

The neutron induced damages of the material for the two modules were simulated and reach up to ~2 dpa/fpy in mirrors, see Fig. 9 and up to ~4 dpa/fpy at EC EPP 2020 design module´s front parts, see Fig. 10.

Out of the analysed cases for the 2019 design, the lowest achieved TFC heating was still 150 W/m^3 maximum, which is by a factor of 3 above the design limit of 50 W/m^3. With the 2020 design results with improved shielding and an increased port side wall were brought down, the values are about 40 W/m^3 and therefore in a safe design region.

As already described there are two port plug modules: a more exposed SM port plug module made of mixture of EUROFER (60%) and water (40%) and FM port plug module that consists of stainless steel (60%) and water (40%). The total power and maximum power densities (neutron and gamma) of these two modules were assessed. The total (neutron and gamma) heating power of the SM port plug module is 2.4 MW while the FM port plug module is heated with 0.74 MW, both values for the 2020 EC EPP design. With this data and also depending on other material properties (e.g. crack-limits), the lifetime of these components can be estimated once the design is more detailed. This shall be further assessed in the conceptual design phase.

Shutdown dose rates (SDDRs) for the DEMO EC equatorial port model have been calculated and are presented in a EUROfusion report [34]. The SDDR inside the EC port has been found for the 2019 model to be dominated by the openings in the port plug plate. The addition of waveguide shields to the model reduced the SDDR in the EC port by nearly an order of magnitude. However, even with the port plug plate acting as a perfect neutron and gamma ray shield and with these waveguide shields in place, the dose rate is above 10^4 µSv/h throughout the port, and in the majority of the cryostat around the port. The 2020 design was also studied meanwhile, and the results are expected soon and are not yet available for this paper.

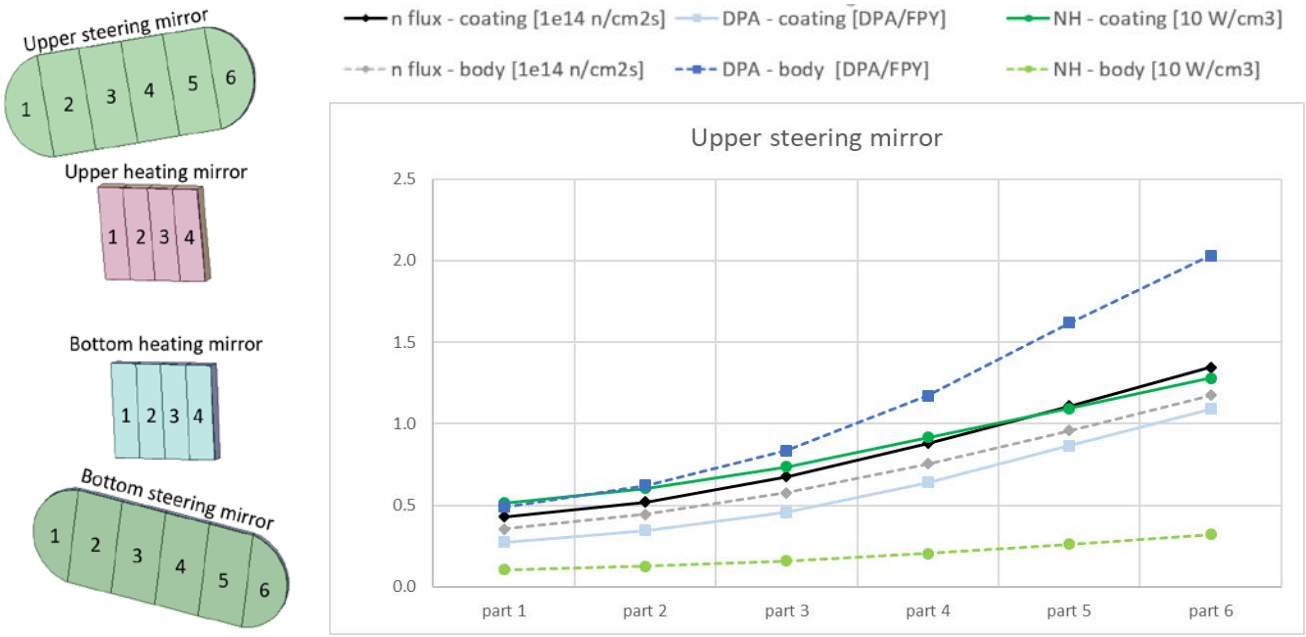

Fig. 9. Nuclear loads in steering and heating mirrors for the 2020 design. Sections of the mirrors studied on the left and as example the plots for the upper steering mirror on the right. NH stands for nuclear heating.

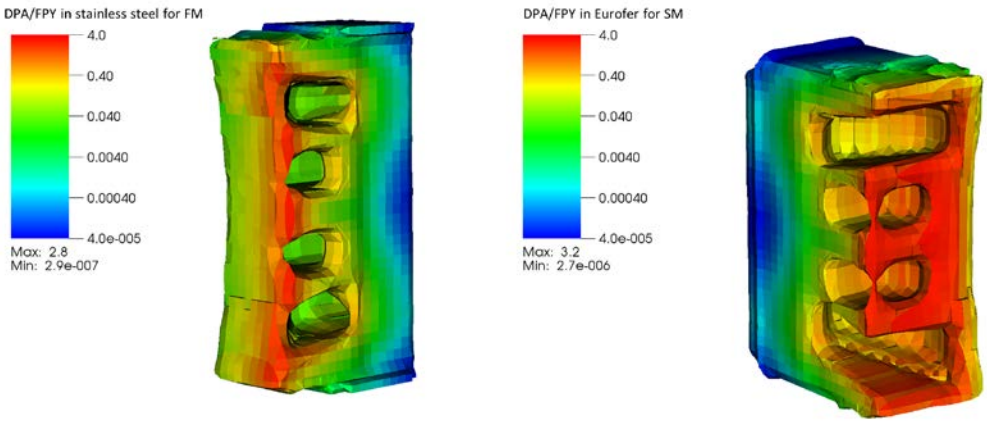

Fig. 10. Neutron induced material damage in units of dpa per full power year for FM (left) stainless steel and SM (right) EUROFER EPP modules, 2020 design.

9.2 Radiative heat loads

First of all, a surface model of the 2020 upgraded design of the EC port was created (Fig. 11, left, red). The surface model of the 2020 upgraded EC port plug required some preparation: re-meshing of critical areas with a modified triangulation was carried out to accommodate for the expected gradients location in the radiation heat load distribution. The computational mesh of the simulation, i.e. the surface over which the radiation heat load was computed, was eventually constituted by this EC port plug only. Still, the remaining EU-DEMO FW components [36] were suitably added to the geometry to have one complete sector (Fig. 11, left, grey). Indeed, FW components were needed as well in the computational environment since radiation could interact with them too. For the same reason, this one sector was repeated 16 times along the toroidal direction to have the complete EU-DEMO vessel.

The radiation source was obtained by suitably merging an ASTRA output power emission distribution (core plasma) [37] and a SOLPS output power emission distribution (scrape-off layer (SOL) plasma) [38]. The overall radiation source in the poloidal section is shown in Fig. 11, right. It was then axis-symmetrically mapped along the toroidal direction to have the complete plasma.

No wavelength-dependence nor reflection from the surfaces were taken into consideration.

The simulation was performed by means of the CHERAB code [39][40]. The post-processing consisted of the improvement of the statistics of the output [41] along with the quantitative inspection of its quality [41][42]. Overall, the result is proved to be accurate and

precise. The two drawings in Fig. 12 have been produced via the software PARAVIEW.

The radiative heat loads are the ones from plasma radiation and reach ~135 kW/m^2 to 170 kW/m^2 inside the BB opening at the side walls, and ~90 kW/m^2 on the EC EPP front surface.

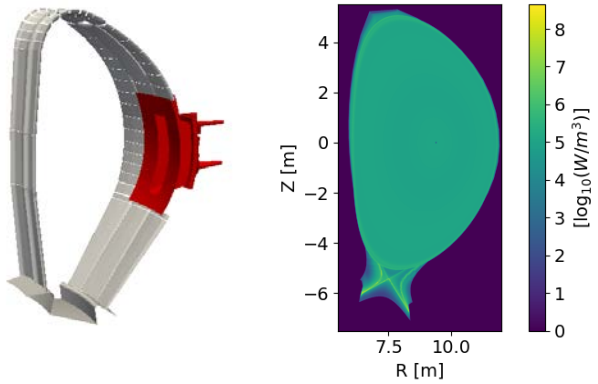

Fig. 11. Input of the simulation of the radiative heat load distribution. Left, geometry of the simulation: 1 out of 16 EU-DEMO sectors composed of the FW (grey) and the EC port plug (red) with all its openings up to the waveguides. Right, radiation source: combination of core and SOL emission.

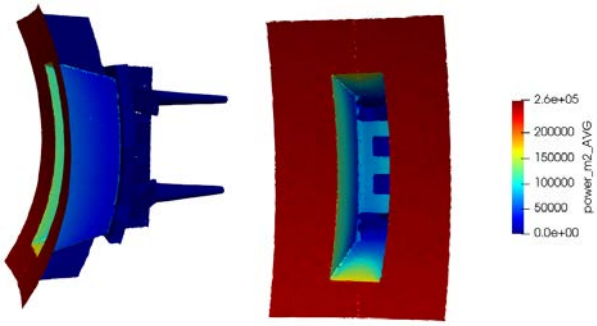

Fig. 12. Surface radiation heat loads up to: (i) ~260 kW/m^2 on the BB FW (consistent with [42]); (ii) ~135 kW/m^2 inside the BB opening side walls (asymmetric); (iii) ~170 kW/m^2 on the lower and upper wall; (iv) ~90 kW/m^2 on the front surface of the port plug.

Also, there is a non-negligible contribution to the focusing steerable and non-steerable mirror surfaces, with 70 kW/m^2 and 40 kW/m^2 respectively, mostly at the mirror sides which are closest to the plasma. On the contrary, the radiative power in the waveguides is negligible with <1 kW/m^2 because no reflections were modelled. However, even if reflection is implemented, this radiative power would be expected to be a minor contribution if compared to microwave transmission and stray radiation losses. Still, reflection could be added in a future step to confirm this assumption also for the quasi-optical system.

9.3 Electromagnetic loads

The electromagnetic loads were studied in 2020 only by analytic calculations. Since they are much higher compared to ITER, the provisional design of the actuators was adapted to it and showed that the actuator and mirror fixations in principle can take the forces and moments of the electromagnetic loads. A more detailed study with electromagnetic simulations will be made in the new framework (Horizon Europe / FP9) starting from 2021 on during the conceptual design phase of DEMO.

9.4 Stray mm-wave radiation loads

The average values from ITER of about 10 kW/m^2 need to be scaled to DEMO and to be added to all exposed surfaces. They are just mentioned here for completeness and need to be accounted for in FP9.

10. Reliability

The required number of ports is derived from simple reliability calculations [43]. These calculations are not based on a detailed failure mode and effects and criticality analysis (FMECA) that would be needed in future to see real mean-time between failure (MBTF) and reliability (r) numbers. For now, a simplified analysis was done, in order to find the best pre-conceptual overall arrangement in terms of number of required spare launchers and waveguides needed in standby. This is a first iteration of the RAMI assessment. This calculation was done for the whole chain: power supplies – gyrotrons – transmission lines – antenna for a clustered approach in order to optimize the overall system reliability.

For comparison of variants of the ECS, a statistical analysis was done for reliability, where the reliability r is defined as $r = e^{(-1/MTBF)}$. The target was defined as >1000 pulses without failure leading to $r_{target} > e^{-0.001}$ which gives an overall system reliability > 99.9%, for each function. The full FMECA is pending as mentioned before but much more complex and not all information are yet available Therefore the given approach gives first ideas on how to setup the system in order to be highly reliably.

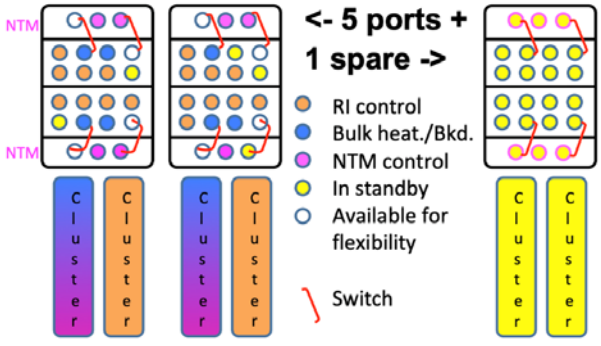

Fig. 13. Variant for the ECS launcher with a total of 6 ports (5 ports and 1 spare port) in a clustered arrangement and the allocated waveguides for the different functions [43].

Table 1 summarizes the results for the chosen variant. A high availability is needed, and for this reason the port plug was designed in a way that the replacement of the M2 mirrors (SMs) is possible without dismantling the waveguides as highlighted in section 7. Also, the figures that are found in [33] give on the mirrors a maximum dpa per fpy of 2.36 dpa, implying 14.2 dpa at DEMO

lifetime, after 6 fpy. If a dpa level of 6 dpa would be assumed for the mirror materials as end of life value, this would mean that one would have to replace the mirrors once in the DEMO lifetime, which would be acceptable in terms of the defined requirements.

Table 1. Results of the statistical analysis for the variant as shown in Fig. 13 to achieve the total power as needed for the provisional physics requirements for each of the functions. Note that the computed statistical reliability r is larger than the value r_{min} = 99.9% mentioned above. The corresponding number of pulses without failure goes from 10'000 to about 1'400, above the requirement. The power assumed below is always in total 130 MW to the plasma, independent of r_{gyro} and the number of gyrotrons remains the same for both cases or gyrotrons reliability.

Number of gyrotrons	108
Gyrotron RF output power	2 MW
Gyrotron reliability r_{gyro}	98 % (95%*)
Total power installed	216 MW
Efficiency gyrotron output to plasma $\eta_{Gyr\text{-}Plas}$	85%
Active Gyrotrons	78
Gyrotrons stand-by	30
Power and reliability for BH	30.6 MW r > 99.99% (> 99.93%)
Power and reliability for NTM control	30.6 MW r > 99.99% (> 99.93%)
Power and reliability for RI control	71.4 MW r > 99,997% (> 99.991%)
Total power to plasma and reliability	**~130 MW** **r > 99.99% (> 99.93%)**

*95% as in ITER, 98% is a target for DEMO

It was also calculated (only for the case r_{gyro} = 98%) how much the reliability would go down if one full EC EPP would fail. In this case the r value drops more drastically from 99.99% to 98.74% (about 80 pulses without failure). Nonetheless this case is assumed to be a rather unlikely event.

11. Conclusion and outlook

An integrated EC EPP design is described as conducted during the pre-conceptual phase in FP8. Starting from the requirements and physics and structural functions, an optical system was designed and around this the EC EPP developed. A split EC EPP is proposed with a steering mirror EPP and a fixed mirror EPP. With first feedback from remote-maintenance, the design was upgraded and will be further elaborated taking into account also electromagnetic loads which are presently under consideration. The present pre-conceptual design of the EC port tried to ease the remote maintainability compared to ITER by producing a pre-conceptual design in which the steering mirror module can be removed and replaced without removing the fixed mirror module and the waveguides. It shall be noted that a significant amount of work is also required to develop this system along with the associated remote maintenance equipment in order to progress to a conceptual design level. That means that a continued collaboration between the WPHCD and work package remote maintenance (WPRM) is essential to allow for the design to be progressed in an integrated manner.

Open issues are the validation of the pre-conceptual design of the actuator, which is outside of the paper to be discussed, a full RAMI FMECA analysis when more details of the design are available, pending SDDR results for the 2020 design, which are assumed to be better than the 2019 results due to better shielding features to be expected soon. Furthermore the building integration needs to get more attention in the FP9 and needs to be improved.

Acknowledgments

This work has been carried out within the framework of the EUROfusion Consortium and has received funding from the Euratom research and training programme 2014-2018 and 2019-2020 under grant agreement No 633053. The views and opinions expressed herein do not necessarily reflect those of the European Commission.

References

[1] Holden, J. et al., DEMO G1 Methodology, EFDA_D_2MY9QF, v2.1

[2] Wu, Ch., HCD-4.2.03-T023-D001 Final report on deliverable Report on the initial investigations on the frequency step-tuning steering concept for DEMO, KIT EFDA_D_2LM9QS, v1.3

[3] Wu, Ch., Basic design considerations for a frequency step-tunable ECCD system to suppress NTMs in DEMO, Fus. Eng. & Design, (2020), submitted

[4] Romanelli, F., EFDA Fusion Roadmap, EFDA_D_2M8JBG, v1.0

[5] Donné, T., et al., European Research Roadmap to the Realisation of Fusion Energy, https://www.euro-fusion.org/index.php?id=61&L=532

[6] Coleman, M., DEMO Power Plant Stakeholder Requirements Document (SHRD), EFDA_D_2MGNEW, v1.0

[7] Bachmann, Ch., DEMO Power Plant Requirements Document (PRD), EFDA_D_2MG7RD, v3.5

[8] DEMO1 Reference Design - 2018, physics baseline documents, EFDA_D_2NLP3X

[9] Siccinio, M. et al., DEMO physics challenges beyond ITER, Fusion Engineering and Design 156 (2020), https://doi.org/10.1016/j.fusengdes.2020.111603

[10] HCD SDR for FP9, EFDA_D_2NV496, v2.0

[11] Federici, G., et al., Overview of the DEMO staged design approach in Europe, Nuclear Fusion, Volume 59, Number 6 (2019), https://doi.org/10.1088/1741-4326/ab1178

[12] Federici, G., et al., DEMO design activity in Europe: Progress and updates, Fusion Engineering and Design, Volume 136, Part A, (2018),

https://doi.org/10.1016/j.fusengdes.2018.04.001
[13] Franke, T., et al., Final Report on Deliverable Integrated design of the DEMO EC port, EFDA_D_2NQWDK, 2020
[14] Siccinio, M., et al., Development of a plasma scenario for the EU-DEMO: current activities and perspectives, submitted for publication in Proceeding of 27th IAEA Fusion Energy Conference, http://www.euro-fusionscipub.org/archives/eurofusion/development-of-a-plasma-scenario-for-the-eu-demo-current-activities-and-perspectives
[15] Palermo, F., Fable, E., Reference Ramp-Up and Ramp-Down trajectories for EU-DEMO and database of plasma perturbations, EFDA_D_2NJ85C, 2020
[16] Bruschi, A. HCD-4.1.06-T018-D001,-D002,-D003,-D004,-D005 Final Report on Deliverables OEWG Antenna for bulk heating (D001) & MBM antenna for bulk heating (D002) & OEWG antenna for NTM control (D003) & MSA for NTM control (D004) & TL routing, losses and component (D005), EFDA_D_2M7ZA9, v1.0, 2020
[17] Bruschi, A, Baiocchi, B., HCD-4.1.06-T020 Interim Report on Deliverables Report on the possibility of the present launchers to deposit power at plasma edge (D001) and feasibility report on the possibility of a modified launcher to deposit power at plasma edge (D002), EFDA_D_2MEKV8, v1.0, 2020
[18] J. Jelonnek, et al., Towards Advanced Fusion Gyrotrons: 2018 Update on Activities within EUROfusion, 2019, The European physical journal / Web of Conferences, 203, 04007, doi:10.1051/epjconf/201920304007
[19] S. Illy, et al., Recent Status and Future Prospects of Coaxial-Cavity Gyrotron Development at KIT., 2019, The European physical journal / Web of Conferences, 203, Art.Nr.: 04005. doi:10.1051/epjconf/201920304005
[20] T.Ruess, et al., Theoretical Study on the Possibility for Stepwise Tuning of the Frequency of the KIT 2 MW 170/204 GHz Coaxial-Cavity Gyrotron, 2020, 45th International Conference on Infrared, Millimeter, and Terahertz Waves (IRMMW-THz), 2020, pp. 1-2
[21] Siccinio, M, Tran, M. Q., Franke, T., Plasma current and toroidal field direction in DEMO, EFDA_D_2P4XMN, v1.0, 2020
[22] Snicker, A., PMI-5.2.2-T005 Final Report on Deliverable ECCD/turbulence interaction in DEMO, EFDA_D_2N3EMQ, v1.1, 2020
[23] Snicker, A., et al., The effect of density fluctuations on electron cyclotron beam broadening and implications for ITER, Nucl. Fusion 58 (2017) 016002, https://iopscience.iop.org/article/10.1088/1741-4326/aa8d07
[24] Henderson, M., et al., Overview of the ITER EC upper launcher, Nucl. Fusion 48 (2008) 054013, https://iopscience.iop.org/article/10.1088/0029-5515/48/5/054013
[25] Poli, E., et al., Electron-cyclotron-current-drive efficiency in DEMO plasmas, Nucl. Fusion 53, No. 1 (2013), https://iopscience.iop.org/article/10.1088/0029-5515/53/1/013011/meta
[26] Schramm, R., Kudlacek, O., Zohm, H., Fable, E., Sauter, E., Poli, E., Janky, F., Treutterer, W., Status of DEMO NTM control, EFDA_D_2NVZEY, v1.0, zip-file, therein ´ntm presentation.pdf´, WPDC Interim Review Meeting Sep 2019
[27] G. Aiello et al., FEM analyses of the ITER EC H&CD torus diamond window unit towards the prototyping activity, Fusion Engineering and Design 161 (2020) 112052
[28] G. Aiello et al., Towards large area CVD diamond disks for Brewster-angle windows, Fusion Engineering and Design 157 (2020) 111818
[29] Franke, T., Spaeh, P., EC EP-EPP Material Definition, EFDA_D_2NQ8G6, v1.0
[30] Bachmann, Ch. PDD - Plant Description Document EFDA_D_2KVWQZ, v1.6
[31] https://ifmifdones.org/
[32] Cufar, A., PMI-3.3-T044-D001 Final Report on MCNP studies 2019, EFDA_D_2P4JQD, v1.3, 2020
[33] Cufar, A., EC port plug neutronic assessment amendment, EFDA_D_2P6UTJ, v1.1, 2020
[34] Berry, T., Eade, T., PMI-3.3-T041-D001 Calculation of ex-VV SDDR, EFDA_D_2NNXAH, v1.1, 2020
[35] Cufar, A., Nuclear analyses of EC port, EFDA_D_2NR9L8, 2020
[36] Gerardin, J., 3D Mesh: VTK, EFDA_D_2NHURS, v2.0
[37] Maviglia, F., TGLF 2017 baseline, EFDA_D_2N75BJ
[38] SOLPS-ITER output, [Online]. Available: on MDSPlus, shot number 111826
[39] M. Carr and A. Meakins, cherab/core: Release v1.1.0, Zenodo, 2019
[40] M. Carr, A. Meakins, A. Baciero and C. Giroud, CHERAB's documentation, 2018, https://cherab.github.io/documentation/index.html
[41] F. Subba and M. Moscheni, Prediction of wall loads during disruptions operation in DEMO, EFDA_D_2NH9BS
[42] F. Subba and M. Moscheni, Prediction of wall loads during steady-state operation in DEMO, EFDA_D_2NDHBC
[43] Rispoli, N., et al., B., HCD-4.1.06-T020-D004 Interim Report on Deliverable Strategy for power sharing between tasks and launchers, with new reliability assessment. (D004), EFDA_D_2NUJ65, 2020